

Application of top seeding in the melt processing of Nd₁₂₃ thick films on YSZ substrates: I buffer layer optimization

M. A. MOUSSA

Physics Department, Faculty of Science, Mansoura University, Mansoura 35516, Egypt

J. S. ABELL, T. C. SHIELDS

School of Metallurgy and Materials, Superconductivity Research Group, University of Birmingham, Birmingham B15 2TT, UK

A new concept of a buffer layer in superconducting thick film technology was tested. The idea is based on increasing the NdBa₂Cu₃O_x melt viscosity at the processing temperature near the substrate by using higher ratios of Nd₄Ba₂Cu₂O_z solid phase in the first screen printed pass which is considered as a buffer layer. Different compositions, thicknesses and thermal schedules were used to optimise the buffer layer. The optimised buffer layer was employed in the fabrication of NdBa₂Cu₃O_y thick films on yttria stabilized zirconia (YSZ) substrates using the top seeding melt growth (TSMG) technique. Using the buffer layer was effective in preventing a large amount of liquid (BaCuO₂-CuO) from severe interaction with the substrate during the prolonged time in the TSMG technique. Consequently, a large superconducting single domain was obtained. Thick films were melt processed in 0.1% O₂ in Ar atmosphere to suppress the Nd_{1+x}Ba_{2-x}Cu₃O_y (Nd_{123SS}) solid solution formation. The produced thick films have high transition temperature (T_C) and improved microstructures.

© 2005 Springer Science + Business Media, Inc.

1. Introduction

The development of thick film technology for high- T_C superconductors (HTS) is particularly important for superconducting applications. Numerous applications are possible for HTS thick films, such as fault current limiters [1, 2] and magnetic shielding [3] which rely on the current carrying characteristics of the film. Other types of applications are devices which depend on the microwave properties (low surface resistance) of the superconductor like antennae [4], resonators [5] and filters [6]. Various coating techniques have been used to fabricate HTS thick films [7, 8]. Among these techniques, screen printing is a low cost and non-vacuum technique and it allows easy patterning on a substrate regardless of its area [9].

In the fabrication of screen printed YBa₂Cu₃O_{7- δ} (YBCO) thick films on YSZ substrates, the interaction layer mainly consists of Ba(Zr_{1-x}Cu_x)O₃ and CuO [10]. In addition, the YBCO system is a stoichiometric compound so the Ba loss did not affect the formation of the Y₁₂₃ high- T_C phase. However, the NdBa₂Cu₃O_x (NdBCO) system is known to form a Nd_{123SS} solid solution due to the fact that the ionic radius of the Nd element is close to that of the Ba [11]. The T_C of the NdBCO system is depressed when trivalent Nd atoms substitute for the divalent Ba site owing to a decrease in the hole or carrier concentration. Consequently, the control of Nd-Ba solid solution during the processing is critical for obtaining the superior superconductor prop-

erties of the NdBCO system in thick film technology. However, some work has been carried out on synthesizing NdBCO superconducting thick thin films by liquid phase epitaxy (LPE) on single crystal substrates [12–14].

Nevertheless, Moussa *et al.* [15, 16] have succeeded in fabricating NdBCO thick films on YSZ substrates with high- T_C and improved microstructure. They have reduced the decomposition temperature (T_P), increased the Ba content in the starting composition and increased the melt viscosity at the processing temperature by the addition of a 10 wt% Nd₄₂₂ secondary phase. They have also increased the ratio of Nd₄₂₂ content to 15 and 20 wt% and the cooling rate was reduced to 10°C/h. This has resulted in obtaining butterfly-like grain with size $\approx 3.5 \times 2.5$ mm² [17]. However, these grains were isolated islands separated by relatively small areas consisting mainly of Nd₄₂₂ phase, BaCuO₂ and CuO. This was the main reason for deteriorating the critical current in these films. This necessitates the application of the top-seeded melt growth (TSMG) technique to obtain a large single superconducting domain without weak links [18]. Consequently, long time at high temperature is needed and slow cooling rates will be used in the application of this technique. Furthermore, the fabrication process of superconducting thick films on any type of substrate includes heating up above the T_P [19]. So there is some type of chemical reaction between the film and substrate, at least for adhesion.

The film/substrate chemical reaction is accompanied by an inevitable shift in composition. Adding this to the complexity in the fabrication of NdBCO bulk materials, the result was that only minor research has been carried out so far on NdBCO thick films [20, 21].

In superconducting thick film technology, several attempts have been made to fabricate a buffer layer to prevent the penetration of harmful ions from the substrates to the superconducting films; the main cause of deteriorating the value of T_C . For example, in the fabrication of YBCO thick films on alumina (Al_2O_3) and sapphire, Bailey *et al.* [22] have fabricated several buffer layers. The first attempt involved the Y_2BaCuO_5 (Y_{211}) and Ba_2CuO_4 on polycrystalline alumina substrates. The Y_{211} produced a powdery layer, which, however, had sufficient adhesion to the substrate. In contrast, the Ba_2CuO_4 layer have melted and formed a completely reacted buffer layer and not merely a film/substrate interface narrow reaction layer. Zero resistance above 77 K was not observed for both types. There was no difference in the reaction between thick films on Al_2O_3 and that produced on either of these two buffer layers for comparable film thickness. In the second attempt, BaZrO_3 would not adhere to the Al_2O_3 substrate over a wide range of high temperatures. The very powdery nature of the buffer layer prevented polishing and therefore was considered unsuitable. Buffer layers were fabricated from $(\text{Ba}_{1-x}\text{Cu}_x)\text{ZrO}_3$, $x = 0.1, 0.2, 0.3, 0.4, 0.5$ using the same heating cycle. The screen printed BaSO_4 with a 10 wt% BaF_2 barrier layer was used in the fabrication of the YBCO thick film on alumina substrates [23]. It was found that the quality of the barrier layer was dependent on the processing temperature. Using reduced firing temperature (950°C) has increased the density of the barrier layer and reduced the diffusion of alumina into the thick films. However, the liquid phases from YBCO thick films leached through some pores in the barrier layer and this has led to the presence of some alumina in the thick films which affected the value of the T_C .

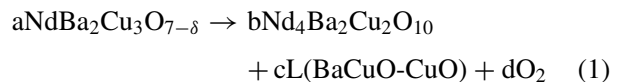
As mentioned above, the use of buffer layers was to prevent the diffusion of Al^{3+} ions and hence the degradation of superconducting properties [24]. However, it has been found that using sintered Nd_{422} instead of alumina substrate is effective in reducing liquid loss during the melt processing of NdBCO bulk [25]. In addition, there are many advantages for using Nd_{422} phase as a buffer layer; for example, it is a part of the peritectic reaction and it is a solid phase at T_P so it increases the melt viscosity during the melt processing.

The preliminary aim of this study is to test a new concept of a buffer layer in thick film technology. The idea is based on increasing the melt viscosity near the substrate by using higher ratios of Nd_{422} phase in the first screen printed pass which is considered as a buffer layer. Different compositions, thicknesses and thermal schedules were used to optimise the buffer layer. The optimised buffer layer was employed in the fabrication of NdBCO thick films on YSZ substrates using the TSMG technique. The final aim is to obtain a large high quality single domain by the application of the TSMG technique.

2. Experimental

The NdBCO precursor was calcined in 1% O_2 in Ar and BaCuO_2 was used instead of BaCO_3 (slow decomposition) to avoid the formation of solid solution in the starting powder as reported elsewhere [15]. The Nd_{123} phase and Ba-rich phase Nd_{422} ($\text{Nd}_{3.6}\text{Ba}_{2.4}\text{Cu}_{1.8}\text{O}_z$) were separately synthesized by solid state reaction. $\text{NdBa}_2\text{Cu}_3\text{O}_y$ phase was prepared by mixing appropriate amounts of Nd_2O_3 , BaCuO_2 and CuO in ethanol using zirconia balls. The dried product was calcined at 820° and 840°C for 12 h under 1% O_2 in Ar with intermediate grinding. The powder was checked for phase purity by XRD and the main phase was Nd_{123} . $\text{Nd}_{3.6}\text{Ba}_{2.4}\text{Cu}_{1.8}\text{O}_z$ was prepared by the same method but calcined at 860 and 900°C for 36 h in 1% O_2 in Ar.

The starting point in this optimisation was mixing Ba-rich phase $\text{Nd}_{3.6}\text{Ba}_{2.4}\text{Cu}_{1.8}\text{O}_z$ with the organic binder (Blythe 63/2) in the ratio 4(solid): 1 (binder) to form ink. A buffer layer from this ink was screen-printed (one screen-printed track $25 \times 15 \text{ mm}^2$) onto YSZ substrates (3 mol% yttria from PI-KEM) with $30 \mu\text{m}$ thickness. This layer was processed at high temperature, as was attempted in the literature [22, 23]. This layer was designed to be BF1. After obtaining unsuccessful results, the attention was paid to the fact that the peritectic reaction is reversible. So, if one component is removed from the reaction, in this case the oxygen, the reaction will proceed in one direction as follows.



On the basis of this information, ink was prepared from $\text{Nd}_{123} + 20 \text{ wt}\% \text{Nd}_{3.6}\text{Ba}_{2.2}\text{Cu}_{1.8}\text{O}_z + 1 \text{ wt}\% \text{CeO}_2$ by combining 4 g with 1 g organic binder and screen-printed onto YSZ substrates to fabricate a $30 \mu\text{m}$ layer (one pass $25 \times 15 \text{ mm}^2$). This buffer layer was named BF2 buffer. Ba-rich Nd_{422} phase was chosen to compensate for the Ba loss in the interaction with the substrate. The addition of 1 wt% CeO_2 was to refine the produced Nd_{422} buffer layer [26, 27].

The $\text{NdBa}_2\text{Cu}_3\text{O}_y + 20 \text{ wt}\% \text{Nd}_{3.6}\text{Ba}_{2.4}\text{Cu}_{1.8}\text{O}_z + 2.5 \text{ wt}\% \text{Ag}_2\text{O}$ were mixed thoroughly in ethanol using zirconia balls. The compositional ratio of Ag_2O was nominated to be 2.5 wt% because it has been found that the melting temperature of NdBCO decreases linearly with the increase in the amount of Ag_2O up to 2.5 wt% under 1% O_2 in Ar, but no further decrease beyond that composition [28]. The dried powder which designed to be Pd20 was mixed with an organic binder by the ratio 4:1 as described before to produce the ink. Thick films from Pd20 ink were screen-printed with a track of $25 \times 15 \text{ mm}^2$ and a green thickness $\approx 90 \mu\text{m}$ (three passes) onto BF2 buffer. MgO single crystal seed $2 \times 2 \text{ mm}^2$ was placed onto the middle of all film surfaces at room temperature (cold seeding) and fixed by a small droplet from the organic binder which was used in the ink production. The thermal schedule is shown in Fig. 1a and its values and thick film nomenclatures are listed in Table I. The temperature was held at 600°C in pure oxygen to burn off the binder for 1.5 h, then,

TABLE I Thermal schedule values for thick films fabricated from Pd20 powder and screen-printed onto BF2 barrier layer

Thick film	T1 (°C)	CR 1 (°C/h)	T2 (°C)	CR 2 (°C/h)	T3 (°C)	CR 3 (°C/h)
Pd20(1)	1020	120	998	10	950	120
Pd20(2)	1020	120	1008	10	958	150
Pd20(3)	1025	180	998	10	958	180

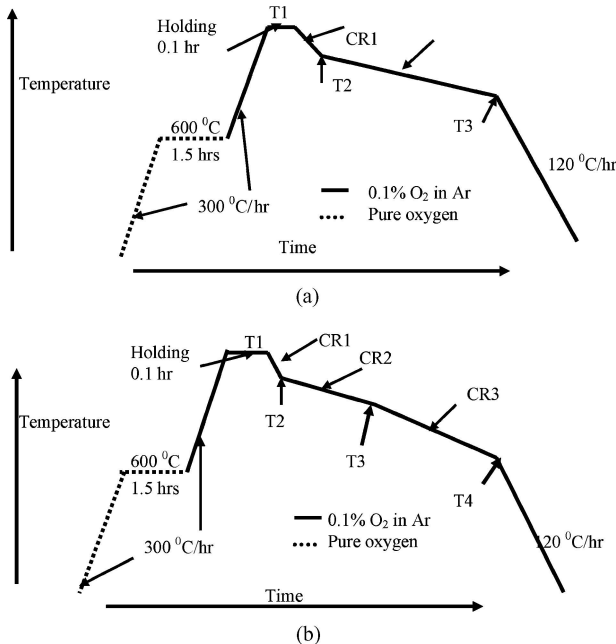


Figure 1 Schematic temperature profiles for thick films prepared from Pd20 and Pd5 powders on BF2 and BF3 Buffer layers, respectively.

the oxygen atmosphere was replaced by 0.1% O₂ in Ar. The temperature was increased to the processing temperature, held for 0.1 h and fast cooled (CR1) to T2. Another slow cooling rate (CR3) was also applied to maximise the controlled grown single domain.

The content of Ba-rich Nd₄₂₂ phase in the buffer layer was increased to 50 wt% and this was called BF3 buffer (NdBa₂Cu₃O_y + 50 wt% Nd_{3.6}Ba_{2.4}Cu_{1.8}O_z, + 1 wt% CeO₂). To investigate the effect of thickness and processing conditions of the buffer on the microstructure and superconducting properties of thick films, ink from BF3 was prepared as above and then one and two passes were screen-printed onto 25 × 15 mm² YSZ substrates with green thickness of 30 and 60 μm, respectively. The buffer layers, before thick film printing, were divided into three groups in the processing, each group consisting of 30 and 60 μm thickness. The first group of buffers was non-sintered (group A). The second group was sintered at 920°C for 0.4 h under 0.1% O₂ in Ar (group B) while the last group was fired at 1000°C for 0.2 h under 0.1% O₂ in Ar (group C). The precursor which was consisted of Nd₁₂₃ + 5 wt% Nd₄₂₂ + 2.5 wt% Ag₂O was mixed and dried as above and called Pd5 powder. Ink from Pd5 powder was prepared as aforementioned. Thick films were screen-printed onto the above three groups of BF3 buffer. MgO single crystal seed was placed onto the middle of all film surfaces as stated early. These films were processed accord-

TABLE II Processing programme values, which was used for BF3 buffer layer optimisation to the thick films fabricated from Pd5 powder

Thick film	T1 (°C)	CR 1 (°C/h)	T2 (°C)	CR 2 (°C/h)	T3 (°C)	CR 3 (°C/h)	T4 (°C)
Pd5A12(1) ^a	1005	100	1000	20	960	–	–
Pd5A22(1) ^b	1005	100	1000	20	960	–	–
Pd5B12(1) ^c	1005	100	1000	20	960	–	–
Pd5B22(1)	1005	100	1000	20	960	–	–
Pd5C12(1) ^d	1005	100	1000	20	960	–	–
Pd5C22(1)	1005	150	980	20	900	–	–
Pd5A12(2)	1005	150	980	20	900	–	–
Pd5A22(2)	1000	150	975	30	900	–	–
Pd5A12(3)	1000	150	975	30	900	–	–
Pd5A22(3)	995	150	980	20	900	–	–
Pd5A12(4)	995	150	980	20	900	–	–
Pd5A22(4)	997	150	980	15	960	20	900
Pd5A12(5)	997	150	980	15	960	20	900
Pd5A22(5)	997	150	980	10	960	20	900
Pd5A12(6)	997	150	980	10	960	20	900
Pd5A22(6)	997	150	975	5	960	20	900
Pd5A12(7)	997	150	975	5	960	20	900

^aA = Non processed BF3, 12 = one layer (30 μm green thickness) of BF3 onto which two layers (60 μm green thickness) of Pd5 powder. The number between the brackets refers to the processing programme of the film.

^b22 = Two screen-printed passes of BF3 onto which two passes from Pd5 powder.

^cB = BF3 processed at 920°C for 0.4 h under 0.1% O₂ in Ar.

^dC = BF3 processed at 1000°C for 0.2 h under 0.1% O₂ in Ar.

ing the thermal schedule in Fig. 1a. As can be seen in Table II, the Pd5A12(1), Pd5A22(1), Pd5B12(1), Pd5B22(1), Pd5C12(1) and Pd5C22(1) films were processed in 0.1% O₂ in Ar with the same heating cycle to investigate the effect of thickness and calcination condition of the buffer layer. According to the microstructure and superconducting properties (see the next section) of the above processed thick films, other thick film series (Pd5A12(2), Pd5A22(2), Pd5A12(3), Pd5A22(3), Pd5A12(4) and Pd5A22(4)) from Pd5 precursor were screen printed onto non-sintered buffer (group A) and the values of the processing programme were changed and also listed in Table II. However, the thermal cycle itself was modified, as schematically shown in Fig. 1b, for other series of thick films (Pd5A12(5), Pd5A22(5), Pd5A12(6), Pd5A22(6) and Pd5A12(7)) which were screen-printed also onto non-sintered buffer; its values were also listed in Table II. The processed thick films were annealed in pure oxygen according to the adopted oxygen annealing programme [15]. In pure oxygen atmosphere, the temperature was raised up to 500°C with a heating rate 300°C/h, held for 1 h, cooled to 300°C at 8°C/h, held for 120 h and then furnace cooled to room temperature.

The superconducting properties of the films were examined using AC susceptibility. The surface and microstructural characteristics of the films were examined by XRD, optical and SEM microscopy with the composition measured by SEM-EDX analysis.

3. Results and discussions

3.1. Buffer layer BF1

It is well known that the T_p of the Nd₄₂₂ phase is higher than that of Nd₁₂₃ phase. Consequently, different

relatively high sintering temperatures were tried to fabricate Nd₄₂₂ (BF1) buffer layers. However, irrespective of sintering temperature, the surface of all sintered BF1 buffer layers were checked by XRD and SEM-EDX analysis and the main phase was Nd₂O₃. This means that all the BaCuO₂ has reacted with the substrate and Nd₂O₃ particles were left. Consequently, the fabrication of Nd₄₂₂ buffer layer on YSZ by this method was unsuccessful.

3.2. Buffer layer BF2

The second trial was the fabrication of the BF2 buffer layer by the peritectic reaction. BF2 was consisted of Nd₁₂₃ + 20 wt% Nd_{3.6}Ba_{2.2}Cu_{1.8}O_z + 1 wt% CeO₂. This barrier layer was heated up to 996°C in 0.041% O₂ in Ar with a heating rate of 300°C/h, held for 0.4 h and cooled to room temperature with a cooling rate of 120°C/h. After sintering, Nd₄₂₂ buffer layer was successfully produced with fine particle sizes. Thick films from Pd20 ink were screen-printed onto the fired BF2 layer according to the thermal schedule in Fig. 1a. Slow cooling rates of 10°C/h were employed between T2 and T3 for ensuring controlled growth around the MgO seed.

From this point, thick films named Pd20(1) to Pd20(3) (see Table I) were processed according to the processing programme schematically drawn in Fig. 1a under 0.1% O₂ in Ar. The difference between the firing condition of the films Pd20(1) and Pd20(2) was the shift of the slow cooling rate (10°C/h) window 10°C higher, but Pd20(3) was processed at 1025°C instead of 1020°C and cooled faster (180°C/h) to 998°C. The

998°C and 958°C values were selected according to the temperature dependence of the oxygen partial pressure (p(O₂)) [29].

Fig. 2 shows the SEM surface images of Pd20(1) film processed at 1020°C in 0.1% O₂ in Ar. As can be noted in Fig. 2a, the film surface is rough compared with the films which were fabricated without barrier layer in a previous work [15]. The grain growth was characterized by the presence of meandering facet lines (Fig. 2b). This could be due to the remaining liquid (BaCuO₂-CuO) from the buffer layer fabrication (see Equation 1), in addition to the liquid from the Nd₁₂₃ film processing. This viewpoint was supported by the presence of trapped liquid in different areas in the film Pd20(1) polished cross section, as can be noted in Fig. 3a. The SEM-EDX analysis of these trapped liquid areas (white areas) was Nd₃Ba₅₇Cu₃₉O_x. Other areas which are shown in Fig. 3b, were distinguished by relatively high-density Nd₄₂₂ particles and comparatively wide interaction layers.

The first clear measure of success in the optimisation should be obtaining high-*T_C* thick films. Although all the films in this series exhibited high onset *T_C*, the susceptibility of each film below *T_C* was considerably different, as shown in Fig. 4. The presence of broad second transition in these films is an indication that they contain clusters of Nd_{1+x}Ba_{2-x}Cu₃O_y solid solution [16]. There are many reasons for the formation of the solid solution given in the literature, introducing the processing at low temperature and/or under high p(O₂) (air or pure oxygen) and the reformation of the NdBCO phase from Ba-deficient liquid [30]. Furthermore, Osamura *et al.* [31] have reported that Nd₄₂₂ tends

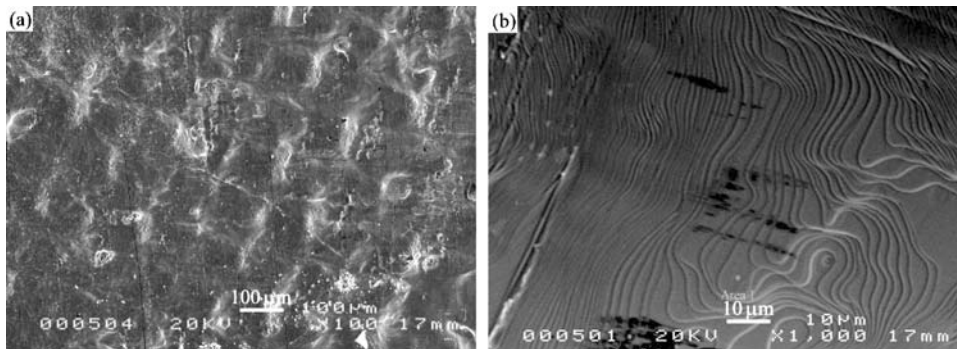


Figure 2 SEM surface images of Pd20(1) thick film on BF2 which was processed at 1020°C in 0.1% O₂ in Ar.

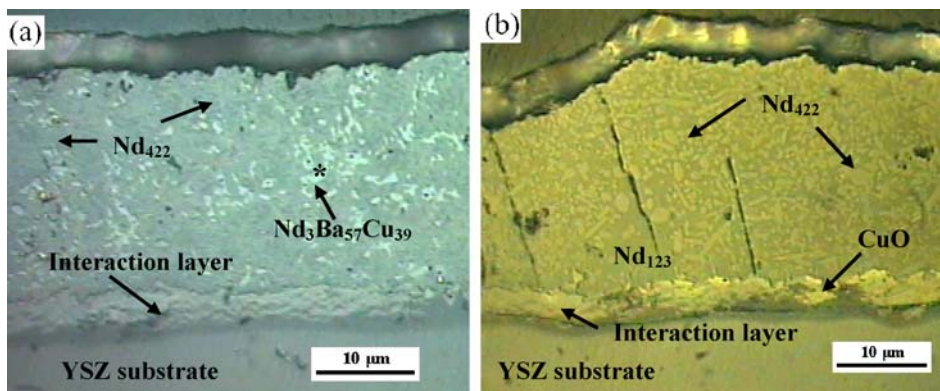


Figure 3 Optical polished cross sections of Pd20(1) film onto BF2 buffer which was fired at 1020°C under 0.1% O₂ in Ar.

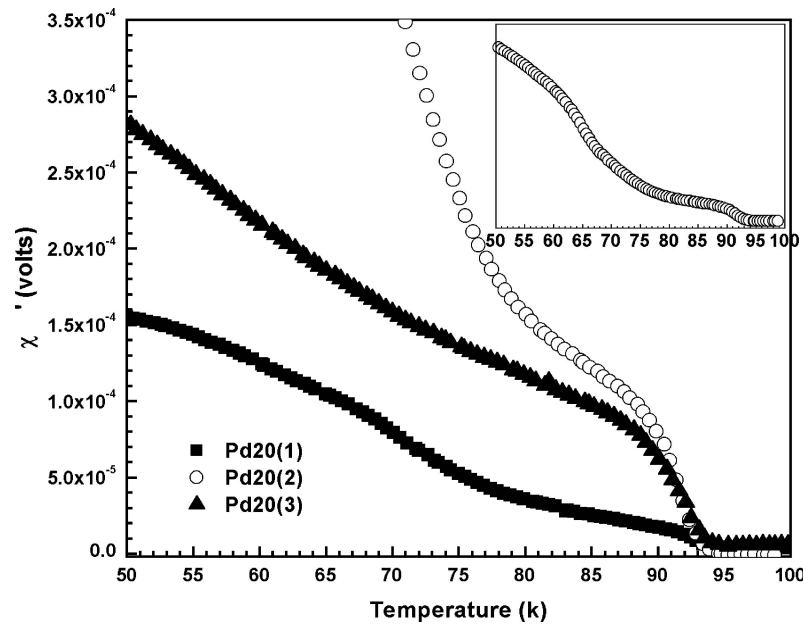


Figure 4 AC susceptibility of thick films screen-printed onto BF2, processed in 0.1% O₂ and annealed in pure O₂ for 120 h. The inset shows the χ'' temperature dependence of Pd20(2) film on different scales.

to form a Ba-rich Nd_{4-y}Ba_{2+y}Cu_{2-y}O_z solid solution. Consequently, the presence of high density of the Nd₄₂₂ phase in Fig. 3b could shift the liquid composition from which the Nd₁₂₃ phase is recombined to the Ba deficient side. This could cause the formation of Nd₁₂₃SS.

3.3. Buffer layer BF3

The application of TSMG to NdBCO bulk superconductor is very difficult due to the formation of solid solution and its undesirable consequences on the T_C and the superconducting transition width [32]. The Nd system has the highest melting point in the 123-family; hence, reducing T_P by a material such as Ag is necessary to be able to use Nd₁₂₃ single crystal as a seed for a good lattice match and in order to avoid the contamination from other seeds, such as MgO single crystals. Moreover, the TSMG implies holding at a high temperature for a long time. The application of TSMG to NdBCO thick films must consider all these parameters. In addition, there are thick film problems such as the film/substrate interaction and the limited quantity of

the processed materials, which implies that any small amount of liquid loss results in considerable change in the film composition and poor superconducting properties.

Bearing these points in mind, with the results of the previous section, a scheme for the experiments in this section may be developed. Firstly, the composition of the barrier layer was shifted to a higher Nd₄₂₂ phase content, compared to the BF2 buffer, to be Nd₁₂₃ + 50 wt% Nd_{3.6}Ba_{2.4}Cu_{1.8}O_y + 1 wt% CeO₂. This buffer was designated to be BF3. Secondly, thick films were fabricated onto this buffer from Nd₁₂₃ + 5 wt% Nd₄₂₂ + 2.5 wt% Ag₂O which were thoroughly mixed and named Pd5.

Ink from Pd5 powder was prepared as aforementioned. Thick films were screen-printed onto the three groups A, B and C of the BF3 buffer as described in Table 8.2. These films and their thermal schedules are shown in Fig. 1b.

For the optimisation of the buffer thickness and sintering conditions, all samples were processed under the same conditions. Fig. 5 shows XRD patterns of thick

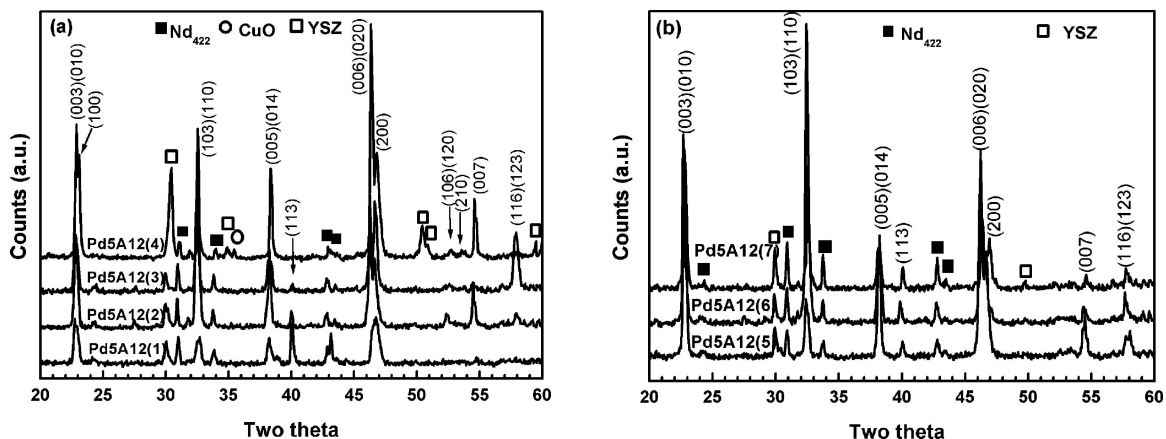


Figure 5 XRD patterns of processed NdBCO thick films fabricated from Pd5 powder. (a) films fabricated on different buffers and thicknesses and (b) the same buffer, but processed at different thermal schedules in 0.1% O₂ in Ar.

films which were fabricated from Pd5 onto BF3 and processed at 1005°C under 0.1% O₂ in Ar. The main phase in the patterns of these films is Nd₁₂₃ which was indexed in the figure. However, different peaks were found and ascribed to the Nd₄₂₂ phase, YSZ substrates and MgO seed. It is important to note that in Fig. 5a the patterns of the films which are fabricated onto two passes BF3 buffer layer, 60 μm, have a better degree of texturing than those fabricated onto one pass of BF3. Fig. 5b shows XRD patterns of thick films fabricated onto non-sintered one pass BF3 as an example. As can be observed in Fig. 5b, the thick film Pd5A12(4) which was processed at 995°C using a slow cooling rate (20°C/h) between 980° and 900°C has the highest degree of *c*-axis texturing. However, there is some degree of *a*-axis texturing, as can be seen from (100) and (200) reflections. It is important to mention that the MgO seed peaks disappeared. This could be due to using a fast cooling rate (150°C/h) between the processing temperature and 980°C and hence reducing the amount of liquid and lower MgO ions diffusion in the processed films.

Fig. 6 shows the SEM surface images of Pd5A12(1), (b) Pd5A12(3), (c) Pd5A12(6) and (d) Pd5A12(7) melt processed thick films. As can be seen, the initial growth took place at the interface between the MgO seed surface and the liquid during the processing. In the micrographs of Pd5A12(1) and Pd5A12(3) (Fig. 6a and b) which were slowly cooled by 20° and 30°C/h respectively, a closer view (higher magnification) showed that the growth around the seed was not a *c*-axis textured platelet. This result agrees with the fact that the growth rate along the *c*-axis is faster than that along *a/b*-axis growth in NdBCO system [33]. By redesigning the processing programme, the growth around the seed for the films Pd5A12(6) and Pd5A12(7) become

approximately 1.4 mm in length. Furthermore, the *c*-axis platelets (*c*-axis normal to the substrate surface) were observed in the growth around the seed as indicated in Figs. 6c and d. It should be stated that at some distance from the seed random nucleation and growth of small grains were also observed. This means that more adaptation for the thermal schedule is needed to enhance the growth around the seed and suppress the homogeneous nucleation further away from it.

Fig. 7 shows the optical micrographs of the polished cross sections of Pd5A12(1), Pd5A22(1), Pd5B12(1), and Pd5C12(1) of processed thick films which were fabricated from Pd5 onto BF3 in 0.1% O₂ in Ar. The micrographs of Pd5A12(1), Pd5A22(1), Pd5B12(1) display twin planes, which indicates the *c*-axis direction of the grown domains [34]. They show also a narrow film/substrate interaction layer, although the temperature was held above 960°C for more than 3 h. Furthermore, in the micrographs of these films, competition growth in two domains can be observed from the twin planes and impurities, such as BaCuO₂-CuO which were pushed between them. It is important to note that the least film/substrate interaction layer was observed for Pd5A12(1) film which was fabricated onto one pass of non-sintered BF3 buffer. So this is one reason for choosing it for further investigation on the effect of changing the thermal schedule. As can be noted in Fig. 7, the density, distribution and sizes of the trapped Nd₄₂₂ particles vary considerably from film to another. The Pd5A12(1) micrograph, Fig. 7a, is free from the Nd₄₂₂ phase, while Pd5A22(1) and Pd5B12(1), Fig. 7b and c, have small Nd₄₂₂ particle sizes which are irregularly distributed. Conversely, the Pd5C12(1) micrograph manifests a wide reaction layer, relatively high density and large trapped Nd₄₂₂ particles.

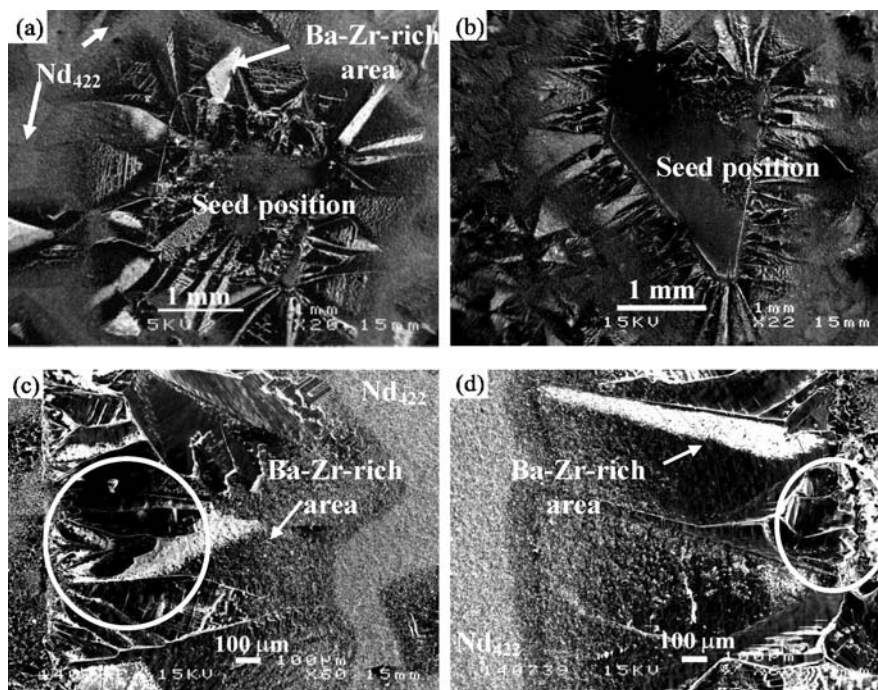


Figure 6 SEM surface images showing the growth around the MgO seed for thick films fabricated from Pd5 powder (a) Pd5A12(1), (b) Pd5A12(3), (c) Pd5A12(6) and (d) Pd5A12(7).

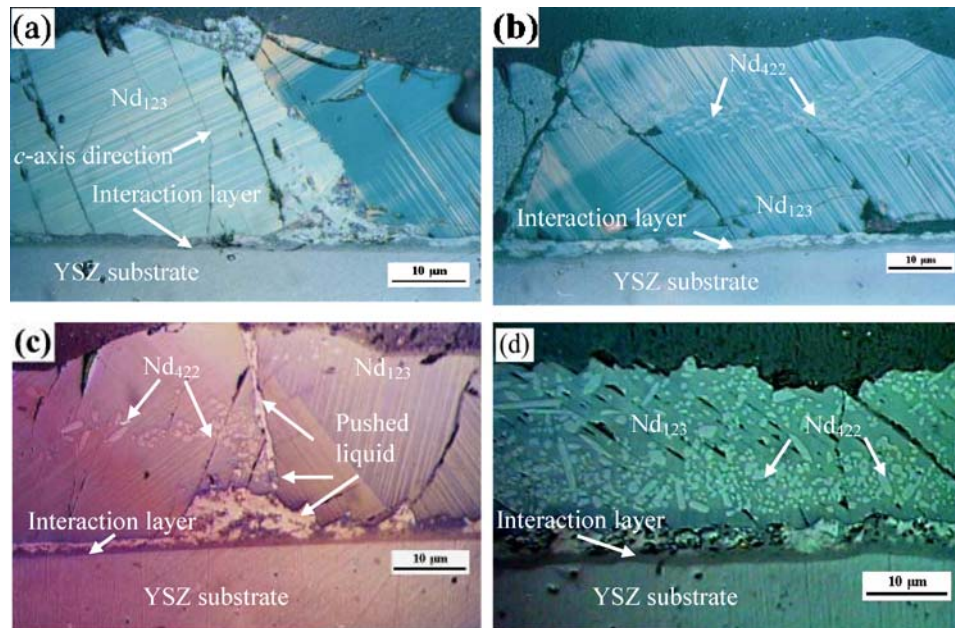


Figure 7 Optical polished cross sections of processed thick films fabricated from Pd5 powder (a) Pd5A12(1), (b) Pd5A22(1), (c) Pd5B12(1) and (d) Pd5C12(1).

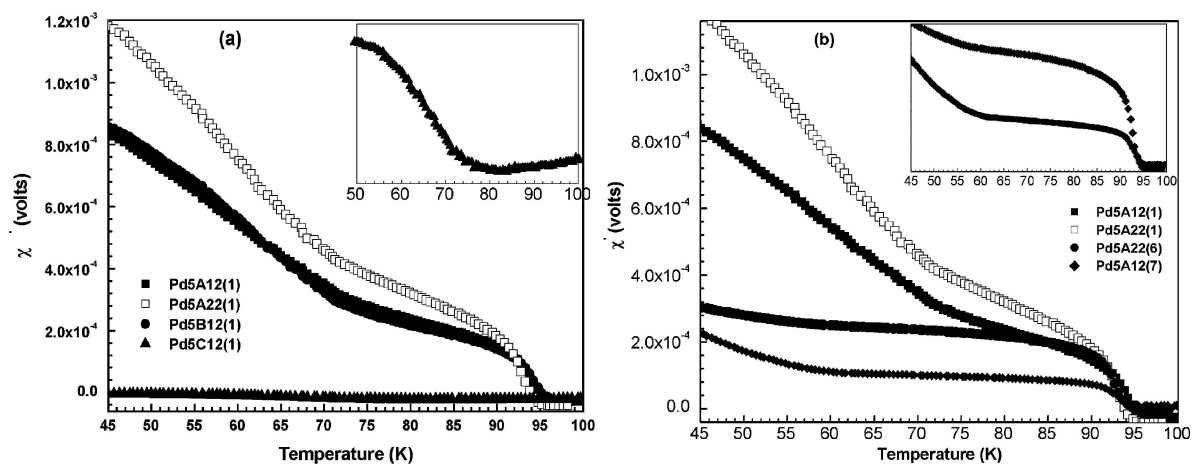


Figure 8 The temperature dependence of χ' of thick films fabricated from Pd5 in 1% O_2 in Ar on BF3 buffer and annealed in pure O_2 .

A high T_C and sharp superconducting transition (small width ΔT_C) should be the first step in the optimisation of thick films fabrication on any buffer or substrate. Fig. 8a shows χ' temperature dependence of processed thick films fabricated on the three buffer types A, B and C in 0.1% O_2 in Ar and oxygen annealed for 120 h. Despite the fact that Pd5A12(1), Pd5A22(1) and Pd5B12(1) films have high- T_C (95 K), they have a second transition at 72 K. Pd5C12(1) has only the second transition at 75 K as shown in the inset of Fig. 8a. The χ' behaviour of Pd5A22(1) can be considered the best one in Fig. 8a. Consequently, films with the same buffer layer compositions (non-sintered) were chosen to study the effect of the processing programme. The nomenclature and thermal schedule of these films are shown in Table II. The two samples Pd5A12(1) and Pd5A12(7) were identical in the layer compositions, but they were processed by different thermal schedules. Furthermore, Pd5A22(1) and Pd5A22(6) films were also have the same layer compositions and dif-

ferent processing programmes. Fig. 8b shows the AC susceptibility of Pd5A12(1), Pd5A22(1), Pd5A12(7) and Pd5A22(6) films which were oxygen annealed for 120 h. The inset in Fig. 8b shows that Pd5A12(7) and Pd5A22(6) have a small second transition between 55 and 60 K. Consequently, changing the processing temperature to be 997°C and using slower cooling rates 10° and 5°C/h between 980° and 960°C were successful in achieving high- T_C and inhibiting the second transition. This can be explained by the fact that $Nd_{1+x}Ba_{2-x}Cu_3O_y$ forms with lower solubility limit (x), which deteriorates the superconducting transition, at higher temperature [30]. As shown, the sintering condition of the buffer layer and the processing programme were affected the superconducting properties and microstructure of the NdBCO thick films. More investigation has been carried out on the optimized (non-sintered) buffer layers and the thermal processing schedule and it will be published under the same title in a second part.

4. Conclusions

Although the Nd₄₂₂ buffer layer was fabricated successfully from Nd₁₂₃ + 20 wt% Nd₄₂₂ powders by utilizing the peritectic reaction, a rough surface and deteriorated superconducting properties for thick films were found. This necessitates more scrutiny of the buffer layer. Superconducting properties and microstructures of thick films fabricated from Pd5 on the non-sintered BF3 buffer were better than those of thick films fabricated on the sintered BF3 buffer. Reducing the liquid viscosity by reducing the decomposition temperature and shorting the holding time before the slow cooling window by using a fast cooling rate were effective in preventing the severe liquid/substrate interaction and producing high-*T_C* thick films. This reflects the importance of using a buffer layer and optimising the processing programme of the thick films.

References

1. D. J. MOULE, P. D. EVANS, T. C. SHIELDS, S. A. L. FOULDS, J. P. G. PRICE and J. S. ABELL, *IEEE Trans. Appl. Supercond.* **7** (1997) 1025.
2. C. MEGGS, G. DOLMAN, T. C. SHIELDS, J. S. ABELL, T. W. BUTTON and F. J. MUMFORD, *IEEE Trans. Appl. Supercond.* **9** (1999) 676.
3. D. B. OPIE, M. E. READ, S. K. REMILLARD, M. J. BROWN, W. J. KOSSLER, H. E. SCHONE, T. W. BUTTON and N. M. ALFORD, *IEEE Trans. Appl. Supercond.* **3** (1993) 189.
4. M. J. LANCASTER, T. S. M. MACLEAN, J. NIBLETT, N. M. ALFORD and T. W. BUTTON, *IEEE Trans. Appl. Supercond.* **3** (1993) 2903.
5. P. A. SMITH, T. W. BUTTON, J. HOLMES, G. DOLMAN and C. MEGGS, *ibid.* **7** (1997) 1763.
6. N. M. ALFORD, S. J. PENN and T. W. BUTTON, *Supercond. Sci. Technol.* **10** (1997) 169.
7. X. QI and J. L. MACMANUS-DRISCOLL, *Current opinion solid St. Mater. Sci* **5** (2001) 291.
8. K. YAMAGIWA, I. HIRABAYASHI, XIULIANG, J. SHIBATA and T. HIRAYAMA, *IEEE Trans. Appl. Supercond.* **9** (1999) 1459.
9. S. PINOL, M. NAJIB, T. PUIG, X. OBRADORS, H. XURIGUERA and M. SEGARRA, *Physica C* **372–376** (2002) 738.
10. M. J. DAY, S. D. SUTTON, F. WELLHOFER and J. S. ABELL, *Supercond. Sci. Technol.* **6** (1993) 96.
11. K. ZHANG, B. DABROWSKI, C. U. SEGRE, D. G. HINKS, I. SHULLER, J. D. JORGENSEN and M. SLAKI, *J. Phys. C: Solid State Phys.* **20** (1987) L935.
12. A. TAKAGI, I. HIRABAYASHI and U. MIZUTANI, *J. Cryst. Growth* **179** (1997) 444.
13. A. TAKAGI, U. MIZUTANI, T. KITAMURA, S. TANIGUCHI, Y. SHIOHARA, I. HIRABAYASHI, S. TANAKA, and Y. YAMADA, *IEEE Trans. Appl. Supercond.* **7** (1997) 1388.
14. Y. NIHORI, Y. YAMADA, Y. YOSHIDA, and I. HIRABAYASHI, *Jpn. J. Appl. Phys.* **11** (1996) L1407.
15. M. A. MOUSSA, J. S. ABELL, and T. C. SHIELDS, *Supercond. Sci. Technol.* **15** (2002) 1467.
16. M. A. MOUSSA, J. S. ABELL, T. C. SHIELDS and K. KAWANO, *ibid.* **16** (2003) 617.
17. M. A. MOUSSA, J. S. ABELL and T. C. SHIELDS, *Mater. Sci. Eng. B*, in Press.
18. N. H. BABU, W. LO, D. A. CARDWELL and Y. SHI, *J. Mater. Res.* **14** (1999) 3859.
19. T. C. SHIELDS, J. B. LANGHORN, S. C. WATCHAM, J. S. ABELL, and T. W. BUTTON, *IEEE Trans. Appl. Supercond.* **7** (1997) 1478.
20. L. DIMESSO, O. B. HYUN and I. HIRABAYASHI, *Physica C* **248** (1995) 127.
21. T. C. SHIELDS, A. RILEY and J. S. ABELL, *Inst. Phys. Conf. Ser.* **158** (1997) 209.
22. A. BAILEY, K. SEALEY, T. PUZZER, G. J. RUSSELL and K. N. R. TAYLOR, *Mater. Sci. Eng. B* **12** (1992) 237.
23. T. C. SHIELDS, J. S. ABELL, A. HUI and A. SMEETS, *Physica C* **213** (1993) 338.
24. T. C. SHIELDS and J. S. ABELL, *Supercond. Sci. Technol.* **5** (1992) 627.
25. S. I. YOO, N. SAKAI, T. TAKAICHI, T. HIGUCHI and M. MURAKAMI, *Appl. Phys. Lett.* **65** (1994) 663.
26. M. MATSUI, N. SAKAI, S. NARIKI, S. J. SEO, and M. MURAKAMI, *Supercond. Sci. Technol.* **13** (2000) 660.
27. H. S. CHAUHAN and M. MURAKAMI, *Mater. Sci. Eng. B* **65** (1999) 48.
28. S. GOSHIMA, N. SAKAI, M. TAKAHASHI, T. HIGUCHI, T. MURAYAMA, K. IIDA, S. I. YOO and M. MURAKAMI, *Adv. Supercond.* **IX** (1996) 739.
29. M. A. MOUSSA, T. C. SHIELDS and J. S. ABELL, *Physica C* **372–376** (2002) 181.
30. W. BIEGER, G. KRABBES, P. SCHATZLE, L. ZELENINA, U. WIESNER, P. VERGES and J. KLOSOWSKI, *ibid.* **257** (1996) 46.
31. K. OSAMURA and W. ZHANG, *Z. Metallkd.* **84** (1993) 8.
32. R. W. MCCALLUM, M. J. KRAMER, K. W. DENNIS, M. PARK, H. WU and R. HOFER, *J. Electron Mater.* **24** (1995) 1931.
33. D. A. CARDWELL, M. KAMBARA, N. H. BABU, P. J. SMITH and Y. SHI, *IEEE Trans. Appl. Supercond.* **11** (2001) 3712.
34. J. D. VERHOEVEN and E. D. GIBSON, *Appl. Phys. Lett.* **52** (1988) 1190.

Received 1 September 2004
and accepted 4 January 2005